A novel penicillin derivative induces antitumor effect in melanoma cells

Viviana Blank[a], Yanina Bellizzi[a], Elsa Zotta[b], Patricia G. Cornier[c],
Carina M.L. Delpiccolo[c], Dora B. Boggián[c], Ernesto G. Mata[c] and
Leonor P. Roguin[a]

In this study, we explored the in-vitro and in-vivo mechanism of antitumor action of a novel synthetic nonantibiotic triazolylpeptidyl penicillin derivative, named TAP7f, on B16-F0 murine melanoma cells. In-vitro assays showed that TAP7f caused an inhibition of S phase progression and a concomitant decrease of the percentage of cells in G_0/G_1 phase. We also found that TAP7f treatment induced an apoptotic response characterized by an increase of the sub-G1 fraction of B16-F0 hypodiploid cells, the occurrence of cells with picnotic nuclei, and the detection of phosphatidylserine exposure on the outer side of the plasma membrane. Apoptotic cell death was further characterized by the activation of caspase-8, caspase-9, and caspase-3; the increase in the proapoptotic/ antiapoptotic ratio of Bcl-2 family proteins; the higher expression levels of Fas receptor and TRAIL ligand; and the cleavage of poly(ADP-ribose) polymerase, a caspase-3 substrate. The in-vivo effect of TAP7f was studied in a syngeneic C57BL/6J mouse melanoma model. Results showed that TAP7f inhibited melanoma cell proliferation in vivo, as determined by a decreased expression of proliferating cell nuclear antigen, inducing a significant reduction of tumor growth. Apoptosis in vivo was assessed by detecting active caspase-3 in tumor slices from treated mice and the expression levels of Fas, TRAIL, and Bcl-2 proteins in tumor lysates. The administration of 80 mg/kg of TAP7f to non-tumor-bearing mice showed no histopathological effects on different organ tissues. Our results suggest that TAP7f might be considered as a potential therapeutic agent for cancer treatment. Anti-Cancer Drugs 00:000–000 Copyright © 2018 Wolters Kluwer Health, Inc. All rights reserved.

Introduction

One of the most important challenges in the treatment of cancer continues being the finding of effective treatments able to reduce death rates and improve quality of life of patients. Among the available treatment options, surgery, radiotherapy, chemotherapy, and immunotherapy still work as valid therapeutic alternatives, although not exempt of some unwanted adverse effects such as toxicity and resistance. In this context, the current problematic requires continuous efforts to find novel, effective, and safer anticancer agents.

Several prescribed antibiotics, such as penicillins, cephalosporins, thienamycins, and monobactams, contain the β-lactam ring as an essential structural feature [1]. Besides the well-known antibacterial properties, the growing interest in the chemistry of β-lactams has opened a novel scenario based on the development of synthetic derivatives with new pharmacological effects, including antitumor activity [2–4]. In this regard, a variety of β-lactam derivatives, such as 7-alkylidene substituted cephems [5], 6-alkylidenepenicillanate sulfones and related 3-alkylidene-2-azetidinones polyaromatic [6] and 1,4-diaryl 2-azetidinones [7,8], N-methylthiolated β-lactams [9,10], 2β-methyl substituted penicillins [11], and ferrocenyl bioconjugates of ampicillin [12], among others, have been reported as potential anticancer agents. In the search of new structural variants with improved anticancer activity, we have recently evaluated the antitumor potency of a library of bicyclic β-lactam derivatives synthesized by molecular hybridization techniques [13]. As a result, a series of new hybrid compounds [triazolyl aminoacyl(peptidyl)penicillins (TAPs)] were obtained by conjugation of penicillin to a peptide via a triazole group. Thus, besides the biological properties of the β-lactam portion, the influence of the 1,2,3-triazole subunit, also found in some cytotoxic drugs, should be considered [14,15]. In addition, the incorporation of the peptide segment could facilitate transport across the cell membranes and/ or achieve effective protein–protein interactions [16,17]. Although TAP7f contains a β-lactam ring, it does not behave as an antibiotic, as it lacks some of the structural characteristics that are essential for the antibacterial

activity of the penicillins, mainly the acylamino group at position 6 of the penam nucleus [18].

When the antiproliferative activity of a series of hybrid compounds was evaluated against HeLa and B16-F0 tumor cell lines, we found that TAP7f, a derivative bearing leucine and phenylalanine bound to the triazole group, showed the most potent and selective cytotoxic action [13]. Based on this finding, in this work, we decided to explore the molecular mechanisms underlying the antitumor action of TAP7f. To this end, after studying a wider panel of human and murine tumor cell lines, we examined the in-vitro ability of this derivative to induce apoptosis in the murine B16-F0 melanoma cell line and then investigated the in-vivo action in a syngeneic C57BL/6J mouse melanoma model.

Materials and methods
Reagents and antibodies
TAP7f was synthesized as described in a previous work [13]. A 100 mmol/l stock solution of the compound was prepared in dimethyl sulfoxide and stored at − 70°C. The stock solution diluted 1/10 in ethanol was used for in-vitro assays at different concentrations in the indicated culture medium. All the experiments were performed with a final concentration of 20 μl vehicle/ml of medium. Caspase substrates Ac-DEVD-AMC (caspase-3), Ac-IETD-AMC (caspase-8), and Ac-LEHD-AMC (caspase-9) were obtained from EMD Millipore (Burlington, Massachusetts, USA). Polyclonal anti-Bax (sc-7480), anti-Bcl-2 (sc-783), anti-Bcl-X_L (sc-1041), anti-Bid (sc-11423), anti-TRAIL (sc-7877), anti-poly(ADP-ribose) polymerase (PARP) (sc-7150), and anti-proliferating cell nuclear antigen (PCNA) (sc-7907) antibodies and monoclonal anti-Fas (sc-8009) were obtained from Santa Cruz Biotechnology Inc (Dallas, Texas, USA). Monoclonal anti-cytochrome C antibody was obtained from BD Biosciences (#556432; San Jose, California, USA). Polyclonal antiactive caspase-3 antibody was obtained from Cell Signaling Technology (#9661; Danvers, Massachusetts, USA).

Cell lines and culture conditions
Except otherwise indicated, cell lines were obtained from the American Type Culture Collection (ATCC, Manassas, USA). Human HeLa (cervix adenocarcinoma, ATCC CCL-2) and HT-1080 cell lines (fibrosarcoma, ATCC CCL-121) were grown in minimum essential medium supplemented with 10% fetal bovine serum (FBS), 2 mmol/l L-glutamine, 50 U/ml penicillin, and 50 μg/ml streptomycin. KB cells (human oropharyngeal carcinoma, ATCC CCL-17) and SK-MEL-28 cells (human malignant melanoma, ATCC HTB-72) were maintained in the same conditions, but adding 1 mmol/l sodium pyruvate/4 mmol/l sodium bicarbonate and 1 mmol/l nonessential amino acids. MCF-7 cell line (human breast cancer, ATCC HTB-22) was cultured in Dubecco's modified Eagle's Medium (Gibco BRL, Gaithersburg, Maryland, USA) containing 4.5 g/l glucose, 1.5 g/l sodium bicarbonate, 10% FBS, 4 mmol/l L-glutamine, 1 mmol/l sodium puyruvate, 0.1 mmol/l nonessential amino acids, 50 U/ml penicillin, and 50 μg/ml streptomycin. B16-F0 (murine melanoma, ATCC CRL-6322), CT26 (murine colorectal carcinoma, ATCC CRL-2638), WM35 (human melanoma, gently supplied by Dr Andras Falus, Department of Genetics, Cell and Immunobiology, Semnelweiss University, School of Medicine, Hungary), HL-60 (human acute promyelocytic leukemia, ATCC CCL-240) and Jurkat cell lines (human acute T cell leukemia, DSMZ ACC-282) were grown in RPMI-1640 (Gibco BRL) supplemented with 10% FBS, 2 mmol/l L-glutamine, 50 U/ml penicillin, and 50 μg/ml streptomycin. NMuMG (normal murine mammary gland, ATCC CRL-1636) and LM3 cells (murine mammary adenocarcinoma), kindly provided by the Institute of Oncology 'Angel H. Roffo' (Buenos Aires, Argentina), were cultured in Dubecco's modified Eagle's Medium-F12 containing 10% FBS, 2 mmol/l L-glutamine, 0.6% HEPES, 50 U/ml penicillin, and 50 μg/ml streptomycin.

Proliferation assay
Cells were incubated in 96-well microplates at a density of 1×10^4 cells/well (KB, B16-F0, HT-1080), 2×10^4 cells/well (HeLa, MCF-7, CT26, LM3, NMuMG), or 5×10^4 cells/well (HL-60, Jurkat) for 72 h at 37°C in the presence of different concentrations of TAP7f or vehicle, in a total volume of 0.2 ml of the corresponding culture medium. Cell number was evaluated by colorimetric determination of the levels of the ubiquitous lysosomal enzyme hexosaminidase [19].

Flow cytometry analyses
To study the effect of TAP7f on cell cycle phase distribution, 5×10^5 B16-F0 cells were incubated for different times at 37°C in the presence or absence of 20 μmol/l of TAP7f in 60 mm Petri dishes. The same protocol was employed to determine the proportion of hypodiploid cells. After treatment, cells were harvested, washed with cold PBS, and then 1×10^6 cells were fixed overnight with 1 ml of 70% cold ethanol and kept at 4°C. To determine the relative DNA content, fixed cells were washed twice with PBS and resuspended in 500 μl of 0.1% sodium citrate buffer, pH 8.4, 0.1% Triton X-100, and 50 μg/ml of propidium iodide (PI). After incubating for 24 h at 4°C, stained cells were analyzed in a FACScanflow cytometer (Becton Dickinson, Franklin Lakes, New Jersey, USA).

Morphological changes visualization
B16-F0 cells (5×10^5) were incubated for 24 h at 37°C in the presence of 20 μmol/l of TAP7f or vehicle in six-well microplates. After harvesting and washing, cells were stained with 50 μg/ml ethidium bromide and 50 μg/ml acridine orange and observed with a fluorescence Olympus BX50 microscope (Olympus America Inc., Center Valley, Pennsylvania, USA) with the corresponding filters (ethidium bromide: 510–550 nm excitation and 590 nm emission wavelengths; acridine orange: 470–490 nm excitation

and 515 nm emission wavelengths). Alternatively, chromatin condensation was visualized after nuclei staining with the blue-fluorescent stain Höechst 33258 (352 nm excitation and 461 nm emission wavelengths).

Annexin V apoptosis assay

B16-F0 cells (5×10^5) were incubated for different times at 37°C in the presence of 20 µmol/l of TAP7f or vehicle in six-well microplates. After harvesting and washing the cells with cold PBS, phosphatidylserine externalization was assessed by Annexin V/PI double staining, according to the manufacturer's instruction (ApoAlert Annexin V-FITC Apoptosis Kit, #630109; BD Biosciences Clontech, San Jose, California, USA). The results were analyzed using a FACScan with WinMDi software (Purdue University Cytometry Laboratories, USA). Annexin $V^+ PI^-$ cells were considered as early apoptotic, whereas Annexin $V^+ PI^+$ cells as late apoptotic/necrotic.

Caspase activity assays

After treatment of B16-F0 cells (6×10^5/ml) for different times with a concentration of 20 µmol/l of TAP7f or vehicle, cells were detached with trypsin/EDTA and washed with cold PBS. Then, 1×10^6 cells were lysed for 30 min at 4°C in 50 µl of lysis buffer (10 mmol/l HEPES, pH 7.4, 50 mmol/l NaCl, 2 mmol/l $MgCl_2$, 5 mmol/l EGTA, 1 mmol/l PMSF, 2 µg/ml leupeptin, and 2 µg/ml aprotinin) followed by three cycles of freezing and thawing. Cell lysates were centrifuged at 17 000g for 15 min, and total protein concentration was determined using Bradford reagent (Bio-Rad, Hercules, California, USA). Aliquots containing 100 µg of protein were diluted in assay buffer (20 mmol/l HEPES, 132 mmol/l NaCl, 6 mmol/l KCl, 1 mmol/l $MgSO_4$, and 1.2 mmol/l K_2HPO_4, at pH 7.4), 20% glycerol, and 5 mmol/l DTT and incubated for 2 h at 37°C with 50 µmol/l of the corresponding fluorogenic substrates (Ac-DEVD-AMC: caspase-3, Z-IETD-7-amino-4-trifluoromethyl coumarin: caspase-8, Ac-LEHD-AMC: caspase-9). Cleavage of the substrates was monitored in a SFM25 Kontron Fluorometer (Kontron Instruments, Milan, Italy). The fluorescence emitted by 7-amino-4-methyl coumarin was measured at 355 nm excitation and 460 nm emission wavelengths, whereas 7-amino-4-trifluoromethyl coumarin was monitored at 400 nm excitation and 505 nm emission wavelengths. Results were expressed as the change in fluorescence units (per µg of protein) relative to control.

Western blotting

B16-F0 cells (6×10^5) were incubated for different times in the presence of 20 µmol/l of TAP7f or vehicle in six-well microplates, harvested, and washed with cold PBS. Then, 1×10^6 cells were lysed for 30 min at 4°C in 10 µl of lysis buffer (10% glycerol, 0.5% Triton X-100, 1 µg/ml aprotinin, 1 µg/ml trypsin inhibitor, 1 µg/ml leupeptin, 10 mmol/l $Na_4P_2O_7$, 10 mmol/l NaF, 1 mmol/l Na_3VO_4, 1 mmol/l EDTA, 1 mmol/l PMSF, 150 mmol/l NaCl, and 50 mmol/l Tris, at pH 7.4). Cell lysates were centrifuged, and aliquots of supernatants containing 100 µg of protein

were resuspended in 0.063 mol/l Tris/HCl, pH 6.8, 2% SDS, 10% glycerol, 0.05% bromophenol blue, and 5% 2-mercaptoethanol; submitted to SDS-PAGE; and transferred onto PVDF membranes (GE Healthcare, Little Chalfont, UK) for 1 h at 100 V in 25 mmol/l Tris, 195 mmol/l glycine, and 20% methanol, at pH 8.2. Membranes were then treated as the usual western blotting method. The secondary antibodies were anti-mouse IgG (horseradish peroxidase-conjugated goat IgG from Santa Cruz Biotechnology; sc-2005) or anti-rabbit IgG (horseradish peroxidase-conjugated goat IgG from Santa Cruz Biotechnology; sc-2004). Immunoreactive proteins were visualized using the Pierce ECL Plus detection system (Thermo Scientific, Waltham, Massachusetts, USA) according to the manufacturer´s instructions. Band intensity was quantified by using a densitometer (Gel Pro Analyzer, Media Cybernetics Inc., Rockville, USA). Mouse anti-tubulin antibody (ab7291; Abcam, San Luis, Missouri, USA) or a rabbit anti-actin antibody (A2066; Sigma-Aldrich, Cambridge, UK) was used to confirm equal protein loading.

Evaluation of mitochondrial membrane potential

To measure $\Delta\Psi$m, B16-F0 cells were treated with 20 µmol/l of TAP7f for 3 h at 37°C. After treatment, cells were detached with trypsin/EDTA, washed twice with cold PBS and incubated with 40 nmol/l of the potential-sensitive cationic lipophilic dye 3, 3′-dihexyloxacarbocyanine iodide [DiOC6(3)] for 20 min at 37°C. Green fluorescence for DiOC6(3) was measured by using a FACScanflow cytometer (Becton Dickinson).

Immunodetection of cytosolic cytochrome *C*

B16-F0 cells were treated with 20 µmol/l of TAP7f for different times, harvested, and centrifuged at 300g for 10 min at 4°C. Cell pellets were washed once with cold PBS, resuspended in 30 µl of sucrose buffer (250 mmol/l sucrose, 20 mmol/l HEPES, pH 7.5, 10 mmol/l KCl, 1.5 mmol/l $MgCl_2$, 1 mmol/l EDTA, 1 mmol/l EGTA, 1 mmol/l dithiotreitol, 0.1 mmol/l PMSF, 1 µg/ml aprotinin, and 1 µg/ml leupeptin), and incubated on ice for 15 min. Cells were then homogenized with a Dounce (40 strokes), and unbroken cells and nuclei were pelleted by centrifugation at 1000g for 10 min. The supernatant was centrifuged at 20 000g for 20 min at 4°C to remove the mitochondrial fraction. The supernatant obtained (cytosolic extract) was stored at −70°C until use. Protein concentration was determined using Bradford reagent, and cytosolic extracts containing 25 µg of protein were loaded onto a 16% SDS-PAGE and then transferred onto PVDF membranes as previously indicated.

In-vivo effect of TAP7f: toxicity studies and tumor growth

All experiments were performed in accordance with the National Institute of Health Guide for the Care and the Use of Laboratory Animals and approved by the Institutional Animal Care and Use Committee (CICUAL) of the School of Pharmacy and Biochemistry, University of Buenos Aires. Female C57BL/6J mice, obtained from the

Animal Care Facility of the School of Veterinary, University of Buenos Aires, were housed in environmentally controlled chambers, with food and water available ad libitum, and were used for experiment at 8–10 weeks old (approximate weight: 20–25 g). To explore if the administration of TAP7f to a group of non-tumor-bearing mice could induce some toxicity, mice were injected intraperitoneally three times per week for 2 weeks with 80 mg/kg of TAP7f or with vehicle. At the end of the treatment, different organs were removed and fixed in formol buffer 10% in PBS 0.1 mol/l, pH 7.4, and then dehydrated and included in paraffin. Cuts of 5 µmol/l were made via microtome (Leica RM 2125; Leica, Wetzlar, Germany) and mounted on 2% xylane-coated slides. Sections were then stained with hematoxylin–eosin for histological analysis. To study the effect of TAP7f on tumor growth, B16-F0 cells (1×10^5) diluted in 200 µl of RPMI were injected subcutaneously in the right flank of each mouse. Following 10–12 days of cell inoculation, mice were divided into four groups: group I (control) received 0.2 ml of vehicle [70% (v/v) polyethylene glycol 400 in PBS]; groups II, III, and IV received 1, 10, and 20 mg/kg, respectively, of TAP7f in vehicle intraperitoneally three times per week for 2 weeks. Animals were daily monitored for overall health status, and their body weights were registered weekly throughout the course of the study. Tumor sizes were measured with a caliper on alternate days, and tumor volumes were calculated using the following formula: $V = (D \times d^2)/2$, where D is the larger diameter and d is the smaller. At the end of the study, mice were anesthetized intraperitoneally with 130 mg ketamine and 13 mg xylazine/kg of body weight, and tumors were excised, weighed, and measured.

Apoptosis-related protein expression in tumors

To evaluate the expression of apoptosis-related proteins, tumors were excised and lysed in a buffer solution containing 10% glycerol, 0.5% Triton X-100, 1 µg/ml aprotinin, 1 µg/ml trypsin inhibitor, 1 µg/ml leupeptin, 10 mmol/l $Na_4P_2O_7$, 10 mmol/l NaF, 1 mmol/l Na_3VO_4, 1 mmol/l EDTA, 1 mmol/l PMSF, 150 mmol/l NaCl, and 50 mmol/l Tris, at pH 7.4. Clear tumor lysate supernatants were obtained by centrifugation and aliquots with 100 µg of protein were resuspended in 0.063 mol/l Tris/HCl, pH 6.8, 2% SDS, 10% glycerol, 0.05% bromophenol blue, 5% 2-mercaptoethanol; loaded onto a 14% SDS-PAGE; and then transferred onto nitrocellulose membranes as indicated before. Bax, Bcl-2, Bcl-X$_L$, and Fas were detected by western blot, and band intensity was quantified by using a densitometer (Gel Pro Analyzer).

Immunohistochemistry

Tumors from mice treated or not with 20 mg/kg of TAP7f were fixed in 10% formaldehyde neutral buffer solution, embedded in paraffin, and sectioned (5 µmol/l) before immunohistochemical analysis. Antigen retrieval was performed by treating tissue sections in 10 mmol/l sodium citrate buffer, pH 6.0, for 50 min at 92°C. Slides were then incubated with antibodies against PCNA or active caspase-3 overnight at 4°C. After rinsing, sections were incubated with a goat anti-rabbit IgG-FITC secondary antibody (sc-2359; Santa Cruz Biotechnology) and observed by fluorescence microscopy.

Statistical analysis

All values are expressed as mean ± SE. P value less than 0.05 was considered statistically significant. Analyses were performed using the GraphPad Prism 5.00 software (GraphPad Software, Inc., California, USA). Statistical analysis of in-vitro data was performed by using the Student's t-test or one-way analysis of variance followed by Dunnett's multiple comparison tests. The effect of TAP7f in mice was analyzed by one-way analysis of variance, and post-hoc comparisons between individual treatments were made using Newman–Keuls multiple comparison tests.
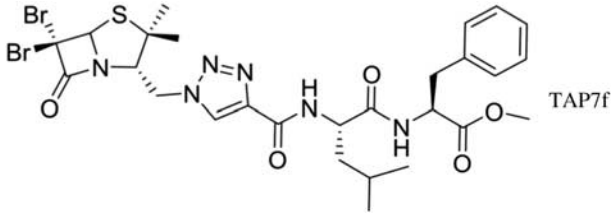
Results

Effect of TAP7f on the proliferation of different cell lines

In a previous work, we evaluated the antiproliferative activity of a library of triazolyl aminoacyl(peptidyl) penicillins against a human (HeLa) and a murine (B16-F0) tumor cell line. Among the tested compounds, the derivative having leucine and phenylalanine bound to the triazole group (TAP7f, see Table 1) showed not only a high antitumor potency but also a good selectivity [13]. Thus, the low cytotoxic effect of TAP7f toward nonmalignant epithelial cells derived from normal mammary gland of mice (NMuMG) indicated a selective action against the tested tumor cells [13]. Herein, we first decided to evaluate the effect of TAP7f in a more extensive panel of human and murine cell lines. The antiproliferative activities, expressed as IC$_{50}$ values, are summarized in Table 1. This table also includes IC$_{50}$ previously obtained in HeLa, B16-F0, and NMuMG cells. Results obtained showed either a high (IC$_{50}$ < 10 µmol/l) or a moderate (IC$_{50}$ ~ 10–20 µmol/l) cytotoxic activity of TAP7f in all the cell lines tested. To characterize the molecular events underlying the antitumor action of TAP7f, we decided to explore the in-vitro mechanism of action on the responsive B16-F0 cell line and its in-vivo antitumor effect in a syngeneic C57BL/6J mouse melanoma model.

TAP7f induces cell cycle arrest and apoptosis in B16-F0 cells

To examine the inhibitory action of TAP7f on B16-F0 proliferation, the effect of TAP7f on cell cycle progression was first examined. B16-F0 cells were incubated in the presence or absence of the synthetic derivative for different times and then analyzed by flow cytometry. As shown in Fig. 1a, the treatment with a 20 µmol/l concentration of TAP7f for up to 18 h caused a decrease of the percentage of cells in G_0/G_1 and an increase in the population of cells in S phase. Thus, after 18 h of incubation with TAP7f, the percentage of cells in G_0/G_1 diminished from 57 ± 3% (control) to 39 ± 3% and the proportion of cells in S phase increased from 32 ± 5%

Table 1 IC$_{50}$ values of TAP7f on different human and murine cell lines

Cell lines	IC$_{50}$ (μmol/l)[a]
Human	
HL-60	3 ± 1
HeLa	3.5 ± 0.3
KB	6 ± 2
HT-1080	7 ± 1
MCF-7	3 ± 1
Jurkat	12 ± 1
SK-MEL-28	17 ± 3
WM35	16 ± 2
Murine	
B16-F0	3 ± 1
CT26	24 ± 3
LM3	18 ± 4
NMuMG	102 ± 8

Results represent the mean ± SE of at least three different experiments.
[a]The molar concentration required to cause 50% growth inhibition (IC$_{50}$) was determined from dose-response curves.

(control) to 48 ± 4%. Furthermore, when B16-F0 cells were incubated for up to 48 h with TAP7f, a time-dependent increment in the sub-G1 population of cells was observed, suggesting that this compound induced an apoptotic response (Fig. 1b). It should be noticed that the high percentage of sub-G1 cells obtained after 24 and 48 h of incubation prevented the study of cell cycle phase distribution at these time periods.

The induction of apoptosis was then confirmed by determining the externalization of phosphatidylserine at the cell surface with Annexin V. When B16-F0 cells were treated with TAP7f for different times, the percentage of early apoptotic cells (AV$^+$PI$^-$) increased from 4 ± 1% (control) to 7 ± 1% and 3 ± 1% (control) to 10 ± 4%, after 6 and 24 h of exposure, respectively, whereas late apoptotic cells (AV$^+$PI$^+$) varied from 7.7 ± 1% (control) to 20 ± 5% and 7 ± 4% (control) to 45 ± 4%, after 6 and 24 h of treatment, respectively (Fig. 2a). Furthermore, after exposing B16-F0 cells to a 20 μmol/l concentration of TAP7f for 24 h, the typical chromatin condensation of apoptotic cells was visualized after staining either with Höechst 33258 or ethidium bromide/acridine orange (Fig. 2b).

Effect of TAP7f on apoptosis-regulating mediators

To explore the intracellular agents contributing to the apoptotic action of TAP7f in B16-F0 cells, we first studied the participation of the executioner caspase-3 and the initiator caspase-8 and caspase-9. As shown in Fig. 3a, caspase-3 proteolytic activity reached a peak (two-fold

increase) after 6 h of exposure to TAP7f, and declined gradually at longer incubation times. A significant activation of both caspase-8 and caspase-9 (~1.5-fold) was also detected after 3 h of treatment, and the activity remained elevated for at least 24 h.

As activation of caspase-9 plays a role in the mitochondrial pathway of apoptosis, we next decided to evaluate the loss of the mitochondrial inner transmembrane potential ($\Delta\Psi_m$) by flow cytometry. A significant decrease of $\Delta\Psi_m$ was observed 3 h after TAP7f exposure, being the percentage of cells with reduced DiOC6(3) incorporation of 30 ± 3 versus 14 ± 3% corresponding to control cells (nontreated cells) (Fig. 3b). In accordance with this result, the significant increase in the cytosolic level of cytochrome C obtained after 3 and 6 h of treatment with TAP7f strongly suggested the release of cytochrome C from mitochondria (Fig. 3c).

Next, we tested whether TAP7f treatment modified the expression levels of some members of the Bcl-2 family proteins. Results obtained in cells exposed to TAP7f for 3 and 6 h showed an increase in the expression levels of Bax and a reduction of the amount of Bcl-X$_L$, Bcl-2, and the full-length Bid protein (Fig. 4). We also found a 2–3-fold increase in TRAIL ligand and Fas receptor levels after 3 h of treatment (Fig. 4). As the PARP, a protein that binds and repairs DNA strand breaks, is also a substrate for caspase-3 [20,21], PARP cleavage was evaluated by western blot assays. As shown in Fig. 4, an almost complete loss of full-length PARP levels was observed 3 and 6 h after treatment of B16-F0 cells with TAP7f.

In-vivo effect of TAP7f on tumor growth

To evaluate whether TAP7f inhibits murine melanoma growth *in vivo*, C57BL/6J mice were subcutaneously inoculated with B16-F0 cells and treated 10–12 days after with vehicle or different doses of the penicillin derivative three times per week for 2 weeks. A dose-dependent effect was evident, being the reduction of tumor volume ~70 and 50% at doses of 20 and 10 mg/kg, respectively, whereas no growth inhibition was observed at 1 mg/kg of TAP7f (Fig. 5a). After treatment with 20 mg/kg of TAP7f, tumor weight diminished ~40% with respect to control group (Fig. 5b). Body weights of TAP7f-treated mice were similar to control during the course of treatment (data not shown). The presence of the cell proliferation marker PCNA was then determined by immunohistochemistry. The expression of PCNA was clearly decreased in 20 mg/kg-treated tumors compared with control (Fig. 5c, top), indicating that TAP7f markedly suppressed melanoma cell proliferation *in vivo*. The histological studies using hematoxylin–eosin staining from 20 mg/kg TAP7f-treated tumor tissues detected the presence of necrotic areas showing unstructured eosinophilic material, nucleus fragments, and cellular debris compared with intact neoplastic proliferation observed as dark purple-stained living cells in control tumor (Fig. 5c, bottom).

Fig. 1

(a)

(b)
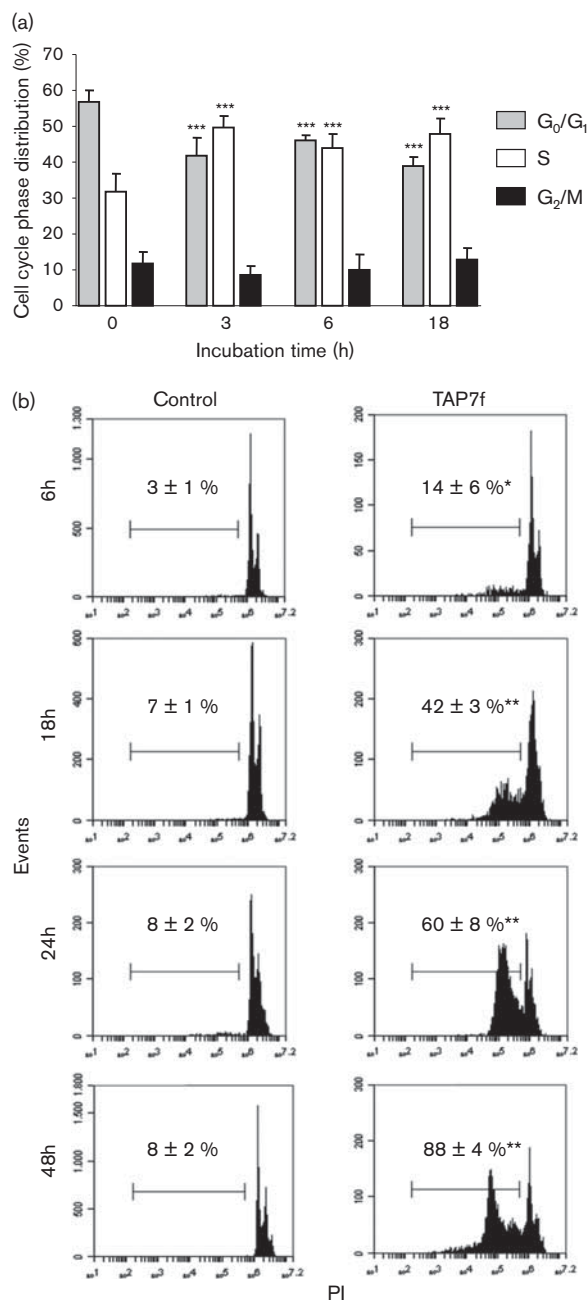
Effect of TAP7f on cell cycle phase distribution and the sub-G1 population of B16-F0 cells. Cells (100 000 cells/ml) were incubated in the absence (control) or presence of 20 μmol/l of TAP7f for different times and then analyzed by flow cytometry. (a) The analysis of DNA content was performed excluding the sub-G1 cell population. Results are mean values ± SE of three different experiments. Control data correspond to cells incubated without TAP7f for 3 h, and similar results were obtained after 6 and 18 h of incubation. Statistical significance in comparison with the corresponding control values is indicated by ***$P < 0.001$. (b) Hypodiploid DNA content was evaluated by flow cytometry after propidium iodide staining as described in the Materials and methods section. The percentage of apoptotic cells ± SE of three different experiments is shown in each histogram. Statistical significance in comparison with the corresponding control values is indicated by *$P < 0.05$, **$P < 0.01$.

Fig. 2

(a)

(b)
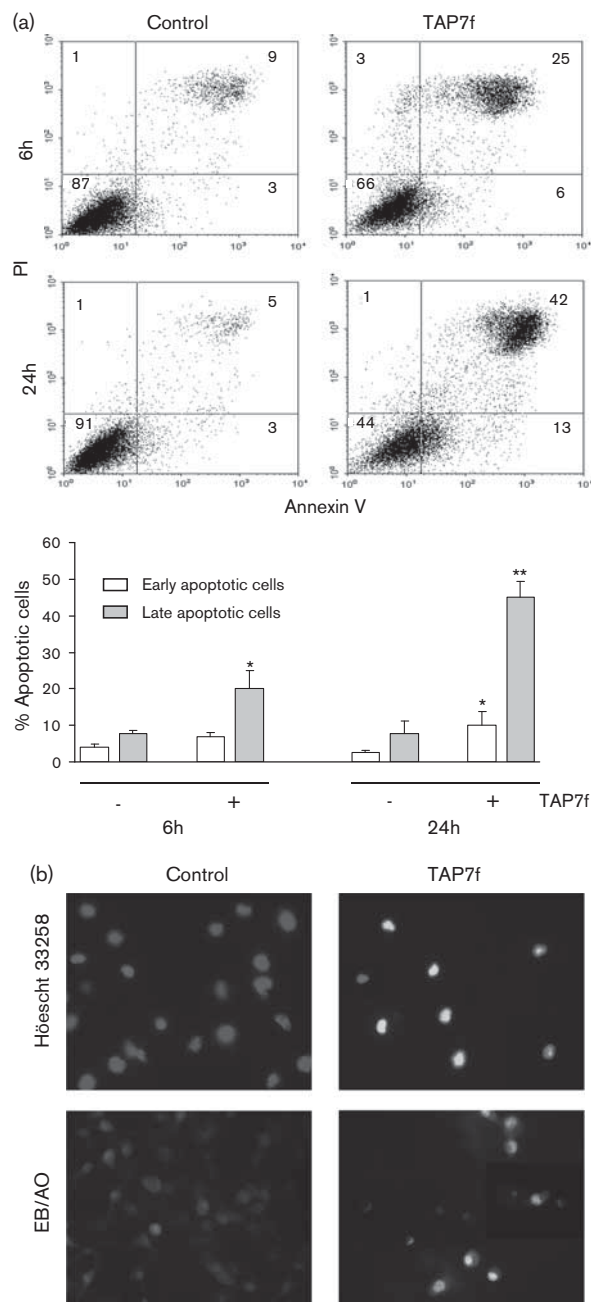
TAP7f-induced apoptotic response in B16-F0 cells. (a) Cells (100 000 cells/ml) were incubated in the absence (control) or presence of 20 μmol/l of TAP7f for 6 and 24 h. After double staining with Annexin V/PI, the apoptotic cell population was evaluated by flow cytometry. Results from one representative experiment are shown (top). Annexin V staining is represented on the x-axis and PI incorporation is represented on the y-axis. Annexin V+PI− cells were considered as early apoptotic cells, whereas Annexin V+PI+ cells as late apoptotic cells. Mean values ± SE of three different experiments are shown in the lower panel. Statistical significance in comparison with the corresponding control values is indicated by *$P < 0.05$ or **$P < 0.01$. (b) After incubating B16-F0 cells in the absence (control) or presence of 20 μmol/l of TAP7f for 24 h, cells were stained with Höechst 33258 or a mixture of ethidium bromide and acridine orange (EB/AO), and visualized with a fluorescence Olympus BX50 microscope (×400).
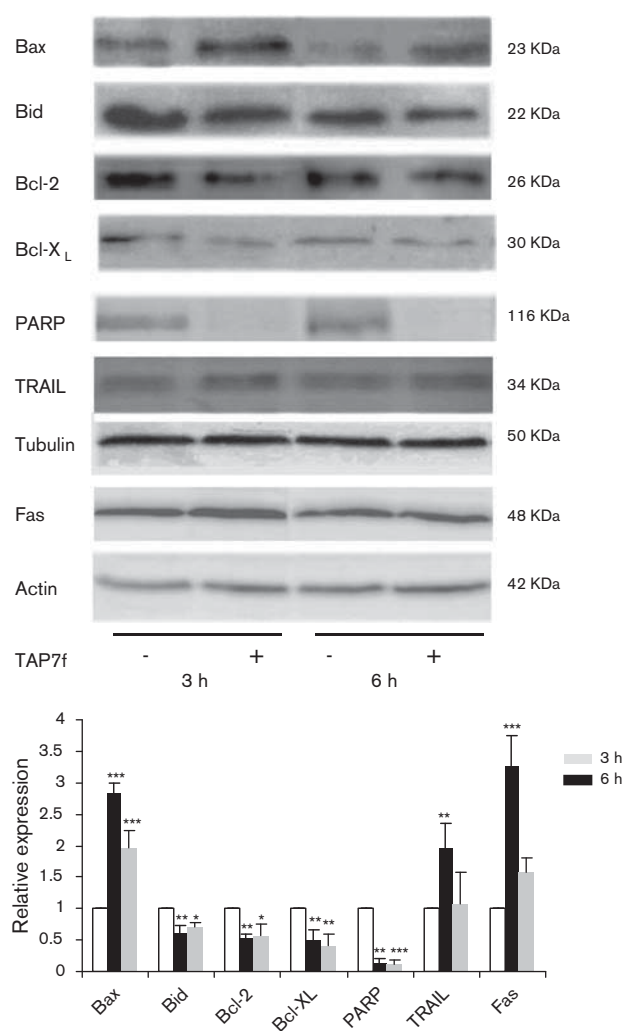
Fig. 3
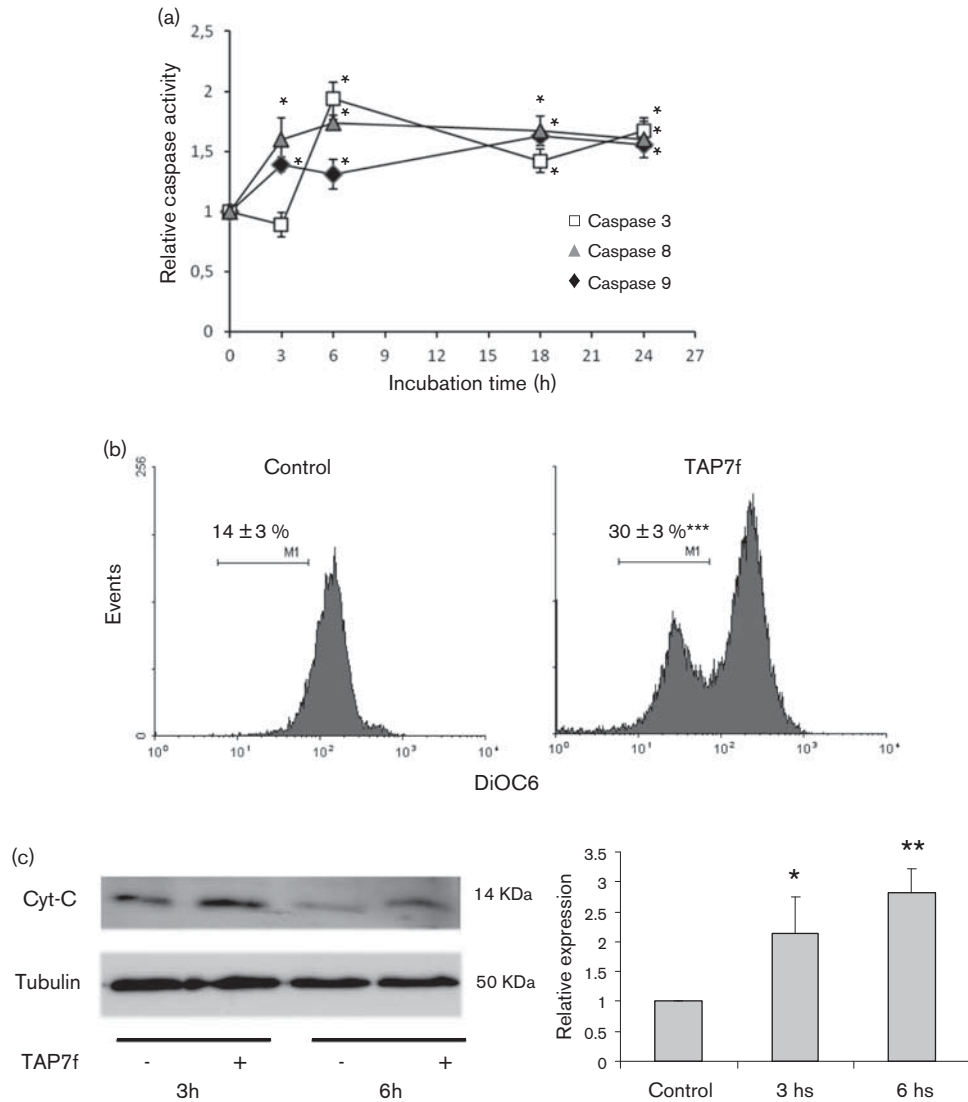
Caspases activation and mitochondrial membrane disruption induced by TAP7f. (a) B16-F0 cells (6×10^5/ml) were incubated for different times in the presence or absence of 20 µmol/l of TAP7f and then caspases activities were determined as indicated in the Materials and methods section. Enzymatic activities are expressed as the ratio of the fluorescence per µg of protein of the treated sample with respect to the fluorescence per microgram of protein of the control and represent mean values ± SE of three different experiments. Statistical significance in comparison with the corresponding control values is indicated by *$P < 0.05$. (b) B16-F0 cells (6×10^5/ml) were incubated for 3 h in the presence or absence of 20 µmol/l of TAP7f, and the mitochondrial membrane potential was measured by flow cytometry after staining the cells with DiOC6(3). Representative histograms of control or Tap7f-treated cells are shown. Statistical significance in comparison with control value is indicated by ***$P < 0.001$. (c) Cytochrome C release was measured by western blot processing of cytosolic extracts obtained from B16-F0 cells treated with 20 µmol/l of TAP7f for 3 and 6 h. Results from one representative experiment are shown (left). Data quantification was performed by densitometric analysis (right). *$P < 0.05$, **$P < 0.01$, significantly different from nonstimulated cells.

The expression of caspase-3 was next detected in tumor cells by immunohistochemistry. As shown in Fig. 6a, higher levels of active caspase-3 were found in tumor cells from 20 mg/kg TAP7f-treated mice with respect to tumors from nontreated mice (control). The expression of different apoptosis-mediator proteins was also evaluated in tumor lysates from mice treated with 20 mg/kg of TAP7f or vehicle (control). Results obtained by western blot showed a significant increment in the expression

levels of Bax (~2-fold), TRAIL (~1.5-fold), and Fas (~3.5-fold) proteins and a decrease in the amount of the full-length Bid protein, Bcl-2, Bcl-X$_L$, and PARP in tumor lysates from treated mice (Fig. 6b).

To further explore whether the administration of TAP7f could induce some toxicity, a group of non-tumor-bearing mice was injected either with vehicle or with 80 mg/kg of TAP7f (a dose four-fold higher than the in-vivo efficient one)

Fig. 4

Bax	23 KDa
Bid	22 KDa
Bcl-2	26 KDa
Bcl-X$_L$	30 KDa
PARP	116 KDa
TRAIL	34 KDa
Tubulin	50 KDa
Fas	48 KDa
Actin	42 KDa

TAP7f   −   +   −   +
         3 h   6 h

Expression levels of Bcl-2 family proteins, PARP, TRAIL, and Fas receptor in cells treated with TAP7f. B16-F0 cells (6×10^5/ml) were incubated for different times in the presence or absence of 20 µmol/l of TAP7f. Total cell lysates were processed for western blot analysis as described in the Materials and methods section. Results from one representative experiment are shown (top). Data quantification was performed by densitometric analysis (bottom). *$P < 0.05$, **$P < 0.01$, ***$P < 0.001$, significantly different from nonstimulated cells.

intraperitoneally three times per week for 2 weeks. Results showed in Fig. 7 revealed that 80 mg/kg of TAP7f did not affect the histological characteristics of different tissues examined after hematoxylin–eosin staining.

Discussion

In an effort to find effective chemotherapeutic agents endowed with selectivity and low toxicity, in this work we first studied the in-vitro antiproliferative activity of TAP7f, a novel synthetic triazolylpeptidyl penicillin derivative, in a panel of different human and murine cell lines, and then examined the mechanism of antitumor action on B16-F0 murine melanoma cells ($IC_{50} = 3 \pm 1$ µmol/l) and the in-vivo effect in a murine melanoma model. We found that TAP7f induced an increase in the population of cells in S phase accompanied by a decrease in G0/G1 phase up to 18 h after treatment. Consistent with our data, Smith et al. [9] reported that an N-thiolated β-lactam derivative induced an inhibition of S phase progression in Jurkat T cells, and a similar behavior was described by Chen et al. [22] in MDA-MB-231 breast cancer cells. In spite of the analogous action shown by these β-lactam derivatives, it should be taken into account that the effect on cell cycle distribution is dependent on both the chemical structure of the compound tested and the cell line assayed [23–27]. In this regard, ceftriaxone, a third-generation cephalosporin antibiotic containing a β-lactam ring, was shown to induce G2/M arrest in a lung tumor cell line [28]. Although these studies with β-lactam antibiotics are included for comparative purposes, it must be considered that TAP7f, although contains a penicillin group in its structure, did not show antibacterial properties (data not shown).

A significant and time-dependent increment in the amount of hypodiploid cells was also observed after 6–48 h of incubation, suggesting that the cell growth inhibitory effect of TAP7f is not only the result of cell cycle arrest but is also related to the induction of an apoptotic response, as it has been previously reported for other β-lactam compounds with anticancer properties [2,10,29,30]. Furthermore, the 1,2,3-triazole subunit is found in some hybrid anticancer drugs inducing an apoptotic cell death [15,31,32].

The apoptosis-inducing property of TAP7f was then confirmed by the detection of apoptotic morphological features, such as the visualization of cells with chromatin condensation and the quantification of phosphatidylserine exposure on the outer side of the plasma membrane, a feature considered a typical early marker of apoptosis [33–35]. The involvement of caspases in the induction of an apoptotic cell death was further studied. It is well-known that the interaction of death receptors with their corresponding ligands promotes the formation of a death-inducing signaling complex that activates the initiator caspase-8. In contrast, caspase-9 is activated after the formation of the apoptosome [36–38]. The cleavage of the effector caspase-3 after activation of the initiator caspases is finally responsible of the typical morphological and biochemical changes that occur during apoptosis [33–38]. Results herein obtained showed that TAP7f induced the activation of initiator caspase-8 and caspase-9 after 3 h of treatment, whereas the activity of the executioner caspase-3 reached a maximal value after 6 h of exposure to TAP7f. Thus, caspase activation kinetics data suggest that both death receptor and mitochondrial pathways would be involved in the apoptotic response triggered by TAP7f. The contribution of the mitochondrial pathway after TAP7f treatment was also

Fig. 5
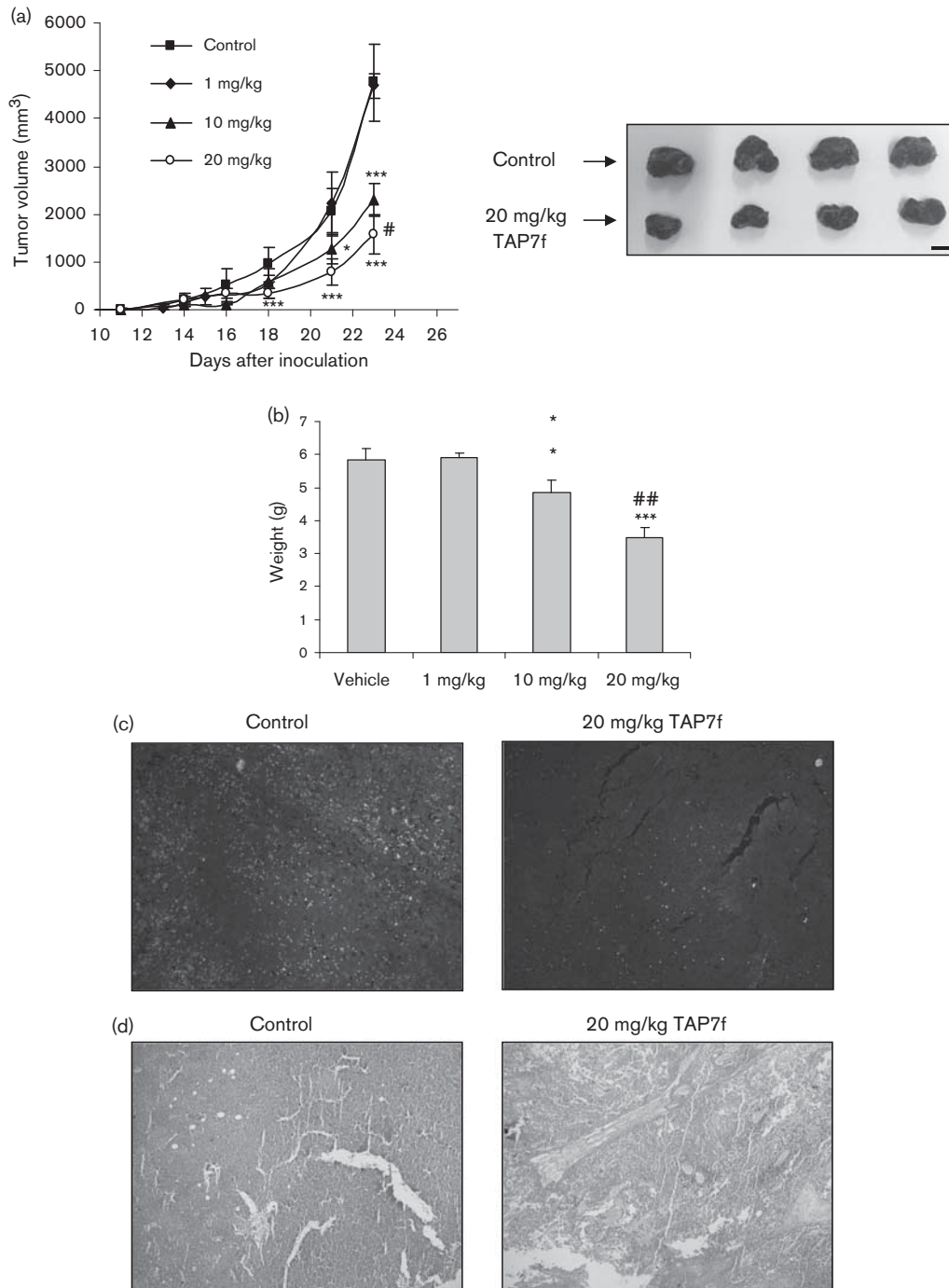
In-vivo effect of TAP7f on melanoma growth. B16-F0 cells (1×10^5) were injected subcutaneously in the right flank of each mouse, and 10–12 days after cell inoculation, mice received vehicle ($n = 20$) or different doses of TAP7f (1 mg/kg, $n = 8$; 10 mg/kg, $n = 8$; 20 mg/kg, $n = 12$) intraperitoneally three times a week for 2 weeks. (a) Tumor sizes were measured with a caliper, and tumor volume was calculated by the formula: $V = (D \times d^2)/2$. Results represent mean values ± SE. Dunnett's multiple comparison test was applied after one-way analysis of variance, *$P < 0.05$, ***$P < 0.001$ respect to control group. Newman–Keuls multiple comparison test after one-way analysis of variance, #$P < 0.05$ respect to 10 mg/kg dose. (b) At the end of the treatment, tumors were excised and the wet weights were measured. ***$P < 0.001$ respect to control group, ##$P < 0.01$ respect to 10 mg/kg dose. (c and d) Tumors from vehicle (control) or 20 mg/kg TAP7f-treated mice were fixed in 10% formaldehyde in PBS and embedded in paraffin. Sections of 5 μm were then revealed by immunofluorescence proliferating cell nuclear antigen staining (c, ×200) or stained with hematoxylin–eosin (d, ×40).

Fig. 6
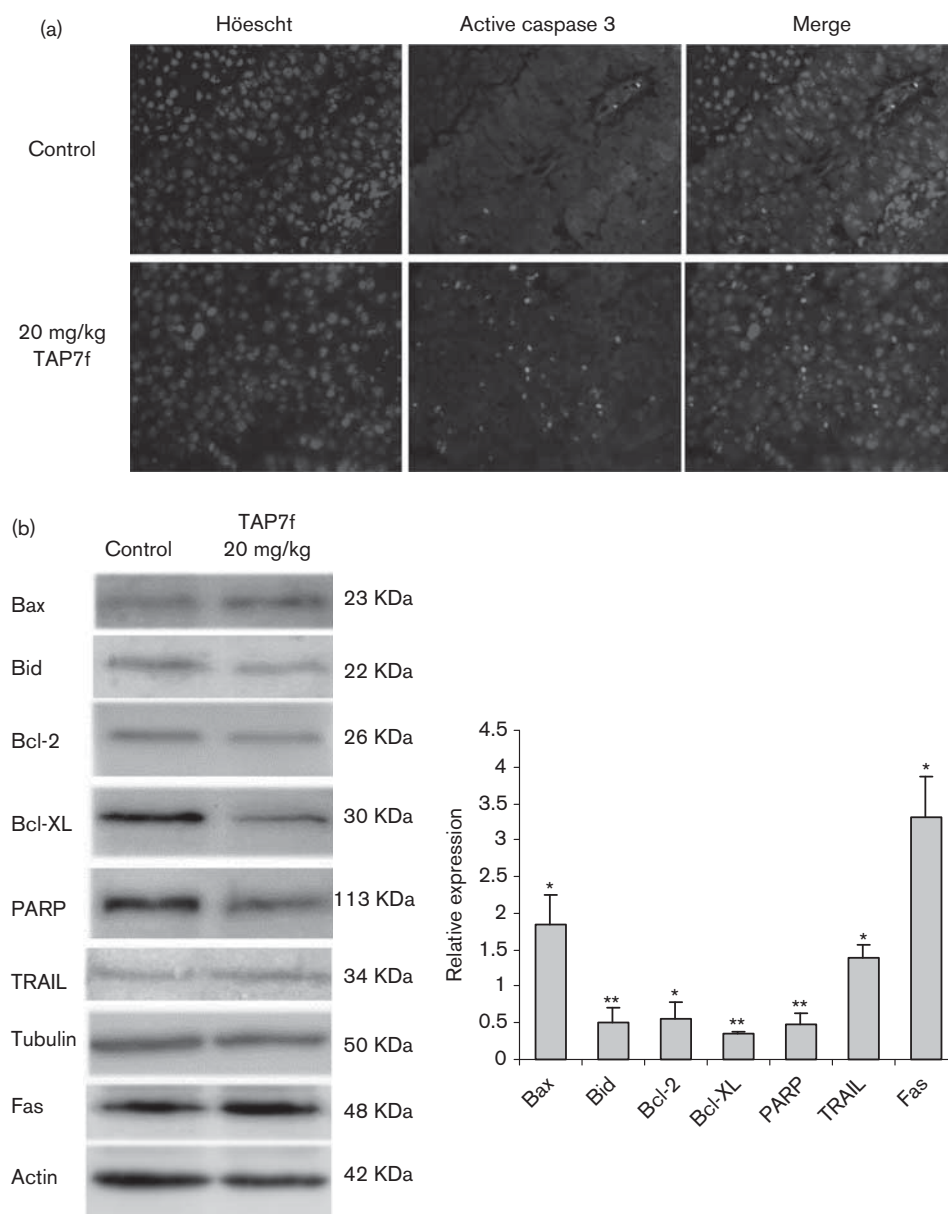
In-vivo induction of apoptosis. (a) Active caspase-3 was analyzed by immunohistochemistry in nontreated tumors (control) and tumors from 20 mg/kg TAP7f-treated mice (×400). Nuclei were stained with Höescht 33258. (b) Levels of Bcl-2 family proteins, PARP, TRAIL, and Fas receptor in cells treated with 20 mg/kg of TAP7f. Tumor lysates were processed for western blot analysis as described in the Materials and methods section. Quantification by densitometric analysis was performed by using Gel Pro software (Media cybernetics Inc., Rockville, USA). Results are expressed as mean ± SE of three different experiments (*$P < 0.05$, **$P < 0.01$, Student's t-test).

assessed by the decrease of the mitochondrial inner transmembrane potential and the release of cytochrome C from the mitochondria, whereas the increase in the expression levels of Fas receptor and TRAIL supported the contribution of the death receptor pathway [33–35]. The expression of Bcl-2 family proteins showed an increase in the ratio of proapoptotic versus antiapoptotic proteins. In addition, it was shown that PARP, a caspase-3 substrate, was cleaved upon TAP7f exposure.

The results obtained *in vitro* encouraged us to explore the in-vivo effect of TAP7f. When C57BL/6J mice challenged with B16-F0 cells were treated with TAP7f, we showed a concentration-dependent reduction of tumor volume. Mice body weight did not decrease during the treatment (data not shown). In addition, the reduction of the expression levels of PCNA in tumor slices obtained from 20 mg/kg-treated mice revealed the ability of TAP7f to inhibit in-vivo cell proliferation. Different

Fig. 7
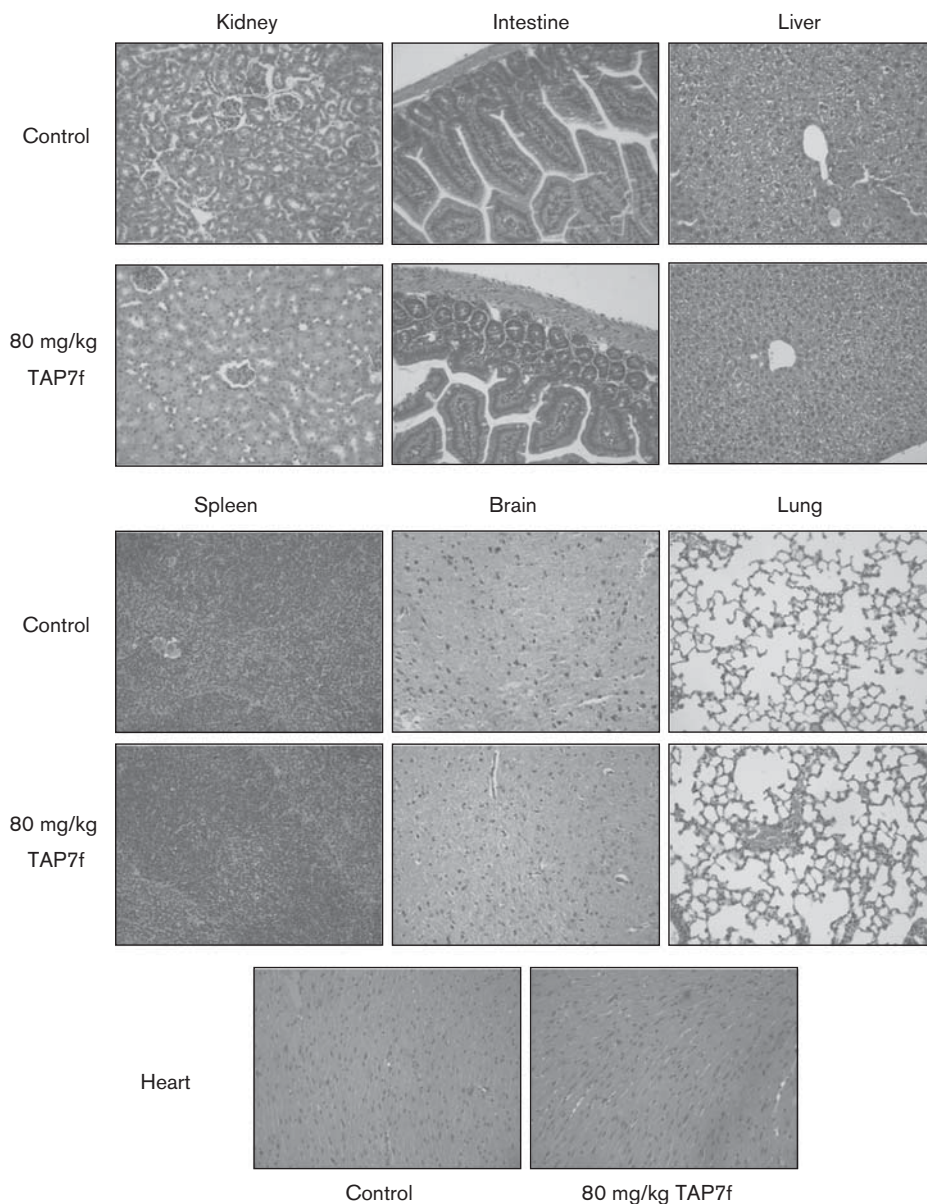
Toxicity studies. Tissues from vehicle (control) or 80 mg/kg TAP7f-treated mice were fixed in 10% formaldehyde in PBS and embedded in paraffin. Sections of 5 μm were then stained with hematoxylin–eosin (×200).

studies have reported the in-vivo antitumor efficacy of other β-lactams compounds, such as *N*-alkylthiolated and *N*-thiolated β-lactams derivatives in breast cancer xeno-grafts [2,22] or ceftriaxone in lung tumor xenografts [28]. However, this is the first time that the antitumor activity of TAP is elucidated *in vivo*. The induction of an in-vivo apoptotic response was also verified after detecting the active form of caspase-3, an increment in the amount of Fas receptor and TRAIL, and a higher ratio of proa-poptotic versus antiapoptotic proteins in tumor lysates from 20 mg/kg-treated mice with respect to control mice. Furthermore, TAP7f did not result to be toxic for other

tissues as no histological differences were observed in different organs extracted from non-tumor-bearing mice injected with vehicle or 80 mg/kg of TAP7f. Thus, after 2 weeks of treatment, no inflammatory infiltrates or hemorrhagic areas were observed in different organs, such as kidney, intestine, liver, spleen, brain, lung, and heart. Previous studies showed the lack of deleterious effect of some β-lactam antibiotics with anticancer prop-erties in both normal cells *in vitro* and animal models [10,30]. Taken together, our results revealed that TAP7f inhibited cell proliferation and induced an apoptotic cell death both *in vitro* and *in vivo*.

Conclusion

The previous screening of a library of triazolyl aminoacyl (peptidyl) penicillins led us to the identification of TAP7f as a selective and potential antitumor agent. Herein, we demonstrated that TAP7f inhibited *in vitro* the proliferation of mouse melanoma cells by arresting cell cycle and inducing an apoptotic response. We also demonstrated the in-vivo efficiency of the penicillin derivative to reduce tumor growth and induce apoptosis through the activation of both death receptor and mitochondria-dependent pathways. In summary, this is the first report describing the antitumor properties of a novel penicillin derivative, which should be considered as a leader and promising therapeutic agent for cancer treatment.

Conflicts of interest

There are no conflicts of interest.

References

1. Alcaide B, Almendros P. Beta-lactams as versatile synthetic intermediates for the preparation of heterocycles of biological interest. *Curr Med Chem* 2004; **11**:1921–1949.
2. Kuhn D, Coates C, Daniel K, Chen D, Bhuiyan M, Kazi A, et al. Beta-lactams and their potential use as novel anticancer chemotherapeutics drugs. *Front Biosci* 2004; **9**:2605–2617.
3. Xing B, Rao J, Liu R. Novel beta-zlactam antibiotic derivatives: their new applications as gene reporters, antitumor prodrugs and enzyme inhibitors. *Mini Rev Med Chem* 2008; **8**:455–471.
4. Vaishnav P, Demain AL. Unexpected applications of secondary metabolites. *Biotechnol Adv* 2011; **29**:223–229.
5. Veinberg G, Vorona M, Shestakova I, Kanepe I, Zharkova O, Mezapuke R, et al. Synthesis and antitumor activity of selected 7-alkylidene substituted cephems. *Bioorg Med Chem* 2000; **8**:1033–1040.
6. Veinberg G, Shestakova I, Vorona M, Kanepe I, Lukevics E. Synthesis of antitumor 6-alkylidenepenicillanate sulfones and related 3-alkylidene-2-azetidinones. *Bioorg Med Chem Lett* 2004; **14**:147–150.
7. Banik I, Becker FF, Banik BK. Stereoselective synthesis of beta-lactams with polyaromatic imines: entry to new and novel anticancer agents. *J Med Chem* 2003; **46**:12–15.
8. O'Boyle NM, Carr M, Greene LM, Bergin O, Nathwani SM, McCabe T, et al. Synthesis and evaluation of azetidinone analogues of combretastatin A-4 as tubulin targeting agents. *J Med Chem* 2010; **53**:8569–8584.
9. Smith DM, Kazi A, Smith L, Long TE, Heldreth B, Turos E, et al. A novel beta-lactam antibiotic activates tumor cell apoptotic program by inducing DNA damage. *Mol Pharmacol* 2002; **61**:1348–1358.
10. Kazi A, Hill R, Long TE, Kuhn DJ, Turos E, Dou QP. Novel N-thiolated beta-lactam antibiotics selectively induce apoptosis in human tumor and transformed, but not normal or nontransformed, cells. *Biochem Pharmacol* 2004; **67**:365–374.
11. Boggián DB, Cornier PG, Mata EG, Blank VC, Cárdenas M, Roguin LP. A solid- and solution-phase-based library of 2β-methyl substituted penicillin derivatives and their effects on growth inhibition of tumor cell lines. *Med Chem Comm* 2015; **6**:619–625.
12. Skiba J, Rajnisz A, de Oliveira KN, Ott I, Solecka J, Kowalski K. Ferrocenyl bioconjugates of ampicillin and 6-aminopenicillinic acid-synthesis, electrochemistry and biological activity. *Eur J Med Chem* 2012; **57**:234–239.
13. Cornier PG, Delpiccolo CM, Mascali F, Boggián DB, Mata EG, Cárdenas M, et al. In vitro anticancer activity and SAR studies of triazolyl aminoacyl (peptidyl) penicillins. *Med Chem Comm* 2014; **5**:214–218.
14. Reddy DM, Srinivas J, Chashoo G, Saxena AK, Sampath Kumar HM. 4β-[(4-Alkyl)-1,2,3-triazol-1-yl] podophyllotoxins as anticancer compounds: design, synthesis and biological evaluation. *Eur J Med Chem* 2011; **46**:1983–1991.
15. Khan I, Guru SK, Rath SK, Chinthakindi PK, Singh B, Koul S, et al. A novel triazole derivative of betulinic acid induces extrinsic and intrinsic apoptosis in human leukemia HL-60 cells. *Eur J Med Chem* 2016; **108**:104–116.
16. Peczuh MW, Hamilton AD. Peptide and protein recognition by designed molecules. *Chem Rev* 2000; **100**:2479–2494.
17. Solcan N, Kwok J, Fowler PW, Cameron AD, Drew D, Iwata S, et al. Alternating access mechanism in the POT family of oligopeptide transporters. *EMBO J* 2012; **31**:3411–3421.
18. Patrick GL. *An introduction to medicinal chemistry*, 5th ed. Oxford, UK: Oxford University Press; 2013. p. 429.
19. Landegren UJ. Measurement of cell numbers by means of the endogenous enzyme hexosaminidase. Applications to detection of lymphokines and cell surface antigens. *J Immunol Methods* 1984; **67**:379–388.
20. Hassa PO, Haenni SS, Elser M, Hottiger MO. Nuclear ADP-ribosylation reactions in mammalian cells: where are we today and where are we going? *Microbiol Mol Biol Rev* 2006; **70**:789–829.
21. Hassa PO, Hottiger MO. The diverse biological roles of mammalian PARPS, a small but powerful family of poly-ADP-ribose polymerases. *Front Biosci* 2008; **13**:3046–3082.
22. Chen D, Falsetti SC, Frezza M, Milacic V, Kazi A, Cui QC, et al. Anti-tumor activity of N-thiolated beta-lactam antibiotics. *Cancer Lett* 2008; **268**:63–69.
23. Kuntz S, Wenzel U, Daniel H. Comparative analysis of the effects of flavonoids on proliferation, cytotoxicity and apoptosis in human colon cancer cell lines. *Eur J Nutr* 1999; **38**:133–142.
24. Joe AK, Liu H, Suzui M, Vural ME, Xiao D, Weinstein IB. Resveratrol induces growth inhibition, S-phase arrest, apoptosis, and changes in biomarker expression in several human cancer cell lines. *Clin Cancer Res* 2002; **8**:893–903.
25. Cho HJ, Yoon Park JH. Kaempferol induces cell cycle arrest in HT-29 human colon cancer cells. *J Cancer Prev* 2013; **18**:257–263.
26. Martinez-Perez C, Ward C, Cook G, Mullen P, McPhail D, Harrison DJ, et al. Novel flavonoids as anti-cancer agents: mechanisms of action and promise for their potential application in breast cancer. *Biochem Soc Trans* 2014; **42**:1017–1023.
27. Choi HJ, Lim DY, Park JH. Induction of G1 and G2/M cell cycle arrests by the dietary compound 3,3′-diindolylmethane in HT-29 human colon cancer cells. *BMC Gastroenterol* 2009; **9**:39.
28. Li X, Li H, Li S, Zhu F, Kim DJ, Xie H, et al. Ceftriaxone, an FDA-approved cephalosporin antibiotic, suppresses lung cancer growth by targeting Aurora B. *Carcinogenesis* 2012; **33**:2548–2557.
29. Greene LM, Nathwani SM, Bright SA, Fayne D, Croke A, Gagliardi M, et al. The vascular targeting agent combretastatin-A4 and a novel cis-restricted {beta}-lactam analogue, CA-432, induce apoptosis in human chronic myeloid leukemia cells and ex vivo patient samples including those displaying multidrug resistance. *J Pharmacol Exp Ther* 2010; **335**:302–313.
30. Bhattacharya B, Mukherjee S. Cancer therapy using antibiotics. *J Cancer Ther* 2015; **6**:849–858.
31. Leu WJ, Swain ShP, Chan SH, Hsu JL, Liu SP, Chan ML, et al. Non-immunosuppressive triazole-based small molecule induces anticancer activity against human hormone-refractory prostate cancers: the role in inhibition of PI3K/AKT/mTOR and c-Myc signaling pathways. *Oncotarget* 2016; **7**:76995–77009.
32. Nagarsenkar A, Guntuku L, Guggilapu SD, Gannoju S, Naidu VG, Bathini NB. Synthesis and apoptosis inducing studies of triazole

linked 3-benzylidene isatin derivatives. *Eur J Med Chem* 2016; **124**:782–793.

33 Hengartner MO. The biochemistry of apoptosis. *Nature* 2000; **407**:770–776.

34 Kaufmann SH, Hengartner MO. Programmed cell death: alive and well in the new millennium. *Trends Cell Biol* 2001; **11**:526–534.

35 Galluzzi L, Vitale I, Abrams JM, Alnemri ES, Baehrecke EH, Blagosklonny MV, *et al.* Molecular definitions of cell death subroutines: recommendations of the

Nomenclature Committee on Cell Death 2012. *Cell Death Differ* 2012; **19**:107–120.

36 Wang C, Youle R. The role of mitochondria in apoptosis. *Annu Rev Genet* 2009; **43**:95–118.

37 Thornberry NA, Lazebnik Y. Caspases: enemies within. *Science* 1998; **281**:1312–1316.

38 Grutter MG. Caspases: key players in programmed cell death. *Curr Opin Struct Biol* 2000; **10**:649–655.